

## Structure of the Sulfuric Acid–Ammonia System and the Effect of Water Molecules in the Gas Phase

Laura J. Larson, Aaron Largent and Fu-Ming Tao\*

Department of Chemistry and Biochemistry, California State University, Fullerton, California 92834

Received: May 7, 1999; In Final Form: July 1, 1999

The proton-transfer reaction of sulfuric acid ( $\text{H}_2\text{SO}_4$ ) and ammonia ( $\text{NH}_3$ ) and the effect of the first two water ( $\text{H}_2\text{O}$ ) molecules were studied by density functional theory and ab initio molecular orbital theory. The equilibrium structures, binding energies, and harmonic frequencies were calculated for each of the three clusters  $\text{H}_2\text{SO}_4\text{--NH}_3\text{--}(\text{H}_2\text{O})_n$  ( $n = 0, 1, 2$ ) using the hybrid density functional (B3LYP) and the second-order Møller–Plesset perturbation approximation (MP2) methods with the 6-311++G(d,p) basis set. Without water ( $n = 0$ ), the  $\text{H}_2\text{SO}_4\text{--NH}_3$  system was determined to be only hydrogen bonded, with  $\text{H}_2\text{SO}_4$  acting as the hydrogen-bond donor and  $\text{NH}_3$  as the acceptor. However, in the presence of one or two water molecules ( $n = 1$  or  $2$ ), the  $\text{H}_2\text{SO}_4\text{--NH}_3$  unit exists only as the  $\text{NH}_4^+\text{·H}_2\text{SO}_4^-$  ion pair that results from a complete proton transfer from  $\text{H}_2\text{SO}_4$  to  $\text{NH}_3$ . The analysis of selected equilibrium bond lengths, binding energies, and harmonic frequencies of the clusters provided strong support for the complete proton transfer in the presence of one or two water molecules. Atmospheric implications of the study are discussed.

### Introduction

Sulfuric acid ( $\text{H}_2\text{SO}_4$ ) and ammonia ( $\text{NH}_3$ ) are two important species in tropospheric chemistry. Atmospheric  $\text{H}_2\text{SO}_4$  is mainly the result of  $\text{SO}_2$  introduced into the air by anthropogenic and natural processes such as the combustion of sulfur-containing fuels and emission from volcanoes. Once in the atmosphere,  $\text{SO}_2$  can be oxidized by hydroxyl radicals and other oxidizing species to form  $\text{SO}_3$  which readily reacts with water molecules to produce  $\text{H}_2\text{SO}_4$ .<sup>1</sup> Natural forms of sulfur, such as DMS and DMDS, are ultimately converted to  $\text{SO}_2$ , which results in additional  $\text{H}_2\text{SO}_4$  production. Ammonia, the only significant base in the atmosphere, is primarily a result of animal wastes,  $\text{NH}_3$ -based fertilizers, and industrial emissions.<sup>2</sup>

The gas-phase reaction of  $\text{H}_2\text{SO}_4$  and  $\text{NH}_3$  is responsible for the creation of sulfur-containing particulates such as  $\text{NH}_4\text{HSO}_4$  and  $(\text{NH}_4)_2\text{SO}_4$ . Along with particulate  $\text{H}_2\text{SO}_4$ , these species represent the three major forms of sulfur-containing aerosols.<sup>3</sup> These particulates play a central role in the formation of cloud condensation nuclei.<sup>4</sup>

It is widely accepted that  $\text{H}_2\text{SO}_4$  will readily and completely react in the aqueous phase with  $\text{NH}_3$  in a standard acid–base neutralization reaction. It is unclear, however, whether a proton transfer from  $\text{H}_2\text{SO}_4$  to  $\text{NH}_3$  will take place in the homogeneous gas phase. No experimental or theoretical evidence is available to support this homogeneous gas-phase proton transfer. What then is the stable form of  $\text{H}_2\text{SO}_4\text{--NH}_3$  in the gas phase? How is the structure of the  $\text{H}_2\text{SO}_4\text{--NH}_3$  unit affected in the presence of water vapor? What is the minimum number of water molecules required to stabilize the  $\text{NH}_4^+\text{·HSO}_4^-$  ion pair? What is the possible role of individual water molecules in transforming the  $\text{H}_2\text{SO}_4\text{--NH}_3$  system into ionic  $\text{NH}_4^+\text{·HSO}_4^-$ ?

Similar problems have been studied for the nitric acid–ammonia ( $\text{HNO}_3\text{--NH}_3$ ) and the hydrogen chloride–ammonia ( $\text{HCl--NH}_3$ ) systems.<sup>5–7</sup> The equilibrium geometries of the

$\text{HNO}_3\text{--NH}_3\text{--}(\text{H}_2\text{O})_n$  ( $n = 0, 1, 2, 3$ ) clusters were determined by ab initio methods.<sup>5</sup> It was found that either without water ( $n = 0$ ) or with one water molecule ( $n = 1$ ), the  $\text{HNO}_3\text{--NH}_3$  system was hydrogen bonded with no proton transfer. Conversely, when two or three water molecules ( $n = 2$  or  $3$ ) were added to the system, a complete proton transfer occurred from  $\text{HNO}_3$  to  $\text{NH}_3$ , resulting in an ion pair.<sup>6</sup> Similar results were obtained for the ammonia–hydrogen chloride system.<sup>7</sup> Proton transfer from  $\text{HCl}$  to  $\text{NH}_3$  did not occur until at least two water molecules were introduced into the  $\text{HCl--NH}_3$  system.

In this paper we report our theoretical results on the  $\text{H}_2\text{SO}_4\text{--NH}_3$  system. Equilibrium structures, binding energies, and vibrational frequencies of the three molecular clusters,  $\text{H}_2\text{SO}_4\text{--NH}_3\text{--}(\text{H}_2\text{O})_n$  ( $n = 0, 1, 2$ ), are calculated using high-level density functional theory (DFT) and ab initio methods. The aim of this study is to seek answers to the questions outlined above. In particular, we wish to explore the molecular structure and properties of the  $\text{H}_2\text{SO}_4\text{--NH}_3$  system with and without water and determine the minimum number of water molecules required to stabilize the  $\text{NH}_4^+\text{·HSO}_4^-$  ion pair that results from a proton transfer from  $\text{H}_2\text{SO}_4$  to  $\text{NH}_3$ . In addition, we wish to test an increasingly popular DFT method and compare it with a traditional ab initio method.

### Theoretical Method

Density functional theory (DFT) and ab initio methods were used to search for the equilibrium geometries of the molecular systems considered and to calculate the molecular properties. The DFT method used in this study was the popular Becke's three-parameter functional<sup>8–10</sup> with the nonlocal correlation provided by Lee, Yang, and Parr (B3LYP).<sup>11</sup> The ab initio method was frozen-core, second-order, Møller–Plesset perturbation approximation (MP2).<sup>12,13</sup> Both of the methods are known to be reliable, particularly for calculations of closed-shell stable molecules and hydrogen-bonded complexes.<sup>14,15</sup> The B3LYP and MP2 calculations were carried out with a reasonably large

\* Author to whom correspondence should be addressed.

basis set, 6-311++G(d,p).<sup>16–18</sup> The reliability of this basis set can be seen in our earlier studies on similar systems.<sup>5–7</sup>

Our molecular clusters,  $\text{H}_2\text{SO}_4\text{--NH}_3\text{--}(\text{H}_2\text{O})_n$  ( $n = 0, 1, 2$ ), were constructed from the three monomeric species ( $\text{H}_2\text{SO}_4$ ,  $\text{NH}_3$ , and  $\text{H}_2\text{O}$ ) whose geometries were optimized at the levels described above. The equilibrium geometries of these clusters were obtained by geometric optimization using analytic gradients. Our primary focus was on the most stable configuration of each cluster, although other configurations with competitive stability were also examined for comparison. Typically, the most stable configuration of a cluster contains the strongest hydrogen bonding between the monomers. For example, the most stable configuration of  $\text{H}_2\text{SO}_4\text{--NH}_3$  is expected to result from a strong hydrogen bond where  $\text{H}_2\text{SO}_4$  acts as the donor of the hydrogen bond and  $\text{NH}_3$  as the acceptor. We only considered this configuration although other, less stable, configurations might exist. For the larger clusters where the most stable configurations could not obviously be determined, additional calculations were performed on the likely candidates to determine the most stable geometry. We will focus our results and discussions on the most stable configuration for each cluster, although less stable configurations will occasionally be mentioned for comparison.

The binding energies of the clusters were also calculated. For a given cluster, the binding energy  $D_e$  was determined as the difference between the total energy of the cluster and the sum of the total energies of the isolated monomers ( $\text{H}_2\text{SO}_4$ ,  $\text{NH}_3$ , and  $\text{H}_2\text{O}$ ) contained in the cluster. The zero-point energy (ZPE) correction based on harmonic vibrational frequencies was considered to give the ZPE-corrected binding energy  $D_0$  of the cluster. Harmonic vibrational frequencies and IR intensities were obtained at the B3LYP/6-311++G(d,p) level for all three clusters and at the MP2/6-31++G(d,p) level for the clusters  $\text{H}_2\text{SO}_4\text{--NH}_3$  and  $\text{H}_2\text{SO}_4\text{--NH}_3\text{--H}_2\text{O}$ . It should be noted that no corrections were made for the basis set superposition error (BSSE) in the calculated binding energy. The BSSE is expected to be relatively small as compared to the binding energy for a strongly hydrogen-bonded system such as  $\text{H}_2\text{SO}_4\text{--NH}_3\text{--}(\text{H}_2\text{O})_n$ . A previous study<sup>5</sup> on a similar system,  $\text{NH}_3\text{--HNO}_3$ , using the same method showed that the BSSE contribution was less than 0.4 kcal/mol, compared to a value of 14 kcal/mol for the binding energy  $D_e$ .

All calculations were carried out with either the *Gaussian 94* or *Gaussian 98* program packages<sup>19–21</sup> on DEC Alpha and IBM RS6000 workstations running Digital UNIX and AIX, respectively.

## Results and Discussion

**Equilibrium Structures.** Figure 1 schematically presents a structure showing the atomic labeling for each of the clusters  $\text{H}_2\text{SO}_4\text{--NH}_3\text{--}(\text{H}_2\text{O})_n$  ( $n = 0, 1, \text{ and } 2$ ). Figure 2 shows a side view of the three-dimensional structure for each of the clusters. Table 1 presents the calculated equilibrium bond distances and angles of the monomeric species,  $\text{NH}_3$ ,  $\text{H}_2\text{SO}_4$ ,  $\text{H}_2\text{O}$ ,  $\text{NH}_4^+$ , and  $\text{HSO}_4^-$ , along with the corresponding experimental values.<sup>22,23</sup> Table 2 presents selected equilibrium bond distances of the three clusters from B3LYP/6-311++G(d,p) and MP2/6-311++G(d,p) calculations. The labeling of the atoms in Figure 1 corresponds to the geometric parameters given in Tables 1 and 2.

As seen in Table 1, the monomer structures from B3LYP and MP2 calculations are comparable and are in reasonable agreement with the experimental structures. Typically, the calculated bond distances are within 0.02 Å of experimental values and the bond angles are within 1° of experimental values.

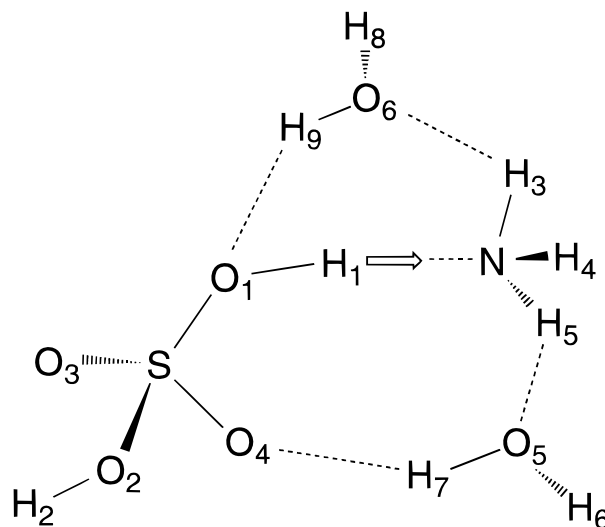


**Figure 1.** A schematic structure representing the most stable configuration of the cluster  $\text{H}_2\text{SO}_4\text{--NH}_3\text{--}(\text{H}_2\text{O})_n$ ,  $n = 2$ . The structures of smaller clusters,  $\text{H}_2\text{SO}_4\text{--NH}_3\text{--H}_2\text{O}$  and  $\text{H}_2\text{SO}_4\text{--NH}_3$ , are represented by consecutively deleting the  $\text{H}_2\text{O}$  molecule with highest atomic label numbers.

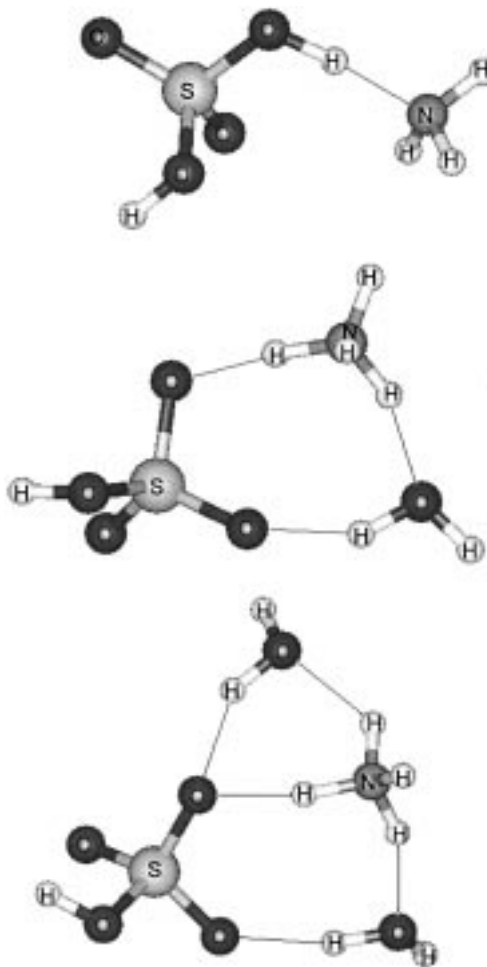


**Figure 2.** A side view of the optimized 3-D structure for each of the clusters  $\text{H}_2\text{SO}_4\text{--NH}_3\text{--}(\text{H}_2\text{O})_n$ ,  $n = 0, 1, 2$ .

It is clear from both Table 2 and Figure 2 that, in the absence of water molecules, the  $\text{H}_2\text{SO}_4\text{--NH}_3$  unit is hydrogen bonded with  $\text{H}_2\text{SO}_4$  acting as the hydrogen-bond donor and  $\text{NH}_3$  as the acceptor. The hydrogen-bond distance,  $r(\text{NH}_1) = 1.586$  Å (B3LYP), is considerably smaller than the hydrogen-bond

**TABLE 1: Equilibrium Bond Distances (in Angstroms), Bond Angles (degrees), Dipole Moments  $\mu$  (D), and Total Energies (Hartrees) Calculated for Monomeric  $\text{NH}_3$ ,  $\text{H}_2\text{SO}_4$ ,  $\text{H}_2\text{O}$ , and  $\text{NH}_4^+$  and  $\text{HSO}_4^-$  from B3LYP and MP2 Calculations with the 6-311++G(d,p) Basis Set**

molecule (symmetry)	parameter <sup>a</sup>	B3LYP	MP2	expt <sup>b</sup>
$\text{NH}_3(\text{C}_{3v})$	$r(\text{NH})$	1.015	1.014	1.012
	$\angle\text{HNH}$	107.9	107.2	106.7
	$\mu$	1.69	1.74	1.51
	$E$	-56.58272	-56.41552	
	$\mu$	3.19	3.63	
$\text{H}_2\text{SO}_4(\text{C}_2)$	$r(\text{O}_1\text{H}_1)$	0.970	0.968	0.97
	$r(\text{O}_2\text{H}_2)$	0.970	0.968	0.97
	$r(\text{SO}_1)$	1.626	1.615	1.422
	$r(\text{SO}_2)$	1.626	1.615	1.422
	$r(\text{SO}_3)$	1.439	1.433	1.574
	$r(\text{SO}_4)$	1.439	1.433	1.574
	$\angle\text{SO}_1\text{H}_1$	109.4	108.8	108.5
	$\angle\text{SO}_2\text{H}_2$	109.4	108.8	108.5
	$\angle\text{O}_1\text{SO}_4$	108.9	109.0	108.6
	$\angle\text{O}_1\text{SO}_3$	105.3	105.1	106.4
	$\angle\text{O}_2\text{SO}_4$	105.3	105.2	106.4
	$\mu$	3.19	3.63	
	$E$	-700.33914	-698.14693	
	$\text{H}_2\text{O}(\text{C}_{2v})$	$r(\text{OH})$	0.962	0.960
$\angle\text{HOH}$		105.0	103.5	104.5
$\mu$		2.16	2.19	1.94
$E$		-76.45853	-76.27492	
$\text{NH}_4^+(\text{T}_d)$	$r(\text{NH})$	1.026	1.024	
	$\angle\text{HNH}$	109.5	109.5	
	$\mu$	0.00	0.00	
	$E$	-56.92036	-56.75569	
$\text{HSO}_4^-$	$r(\text{O}_2\text{H}_2)$	0.965	0.964	
	$r(\text{SO}_1)$	1.470	1.462	
	$r(\text{SO}_2)$	1.714	1.700	
	$r(\text{SO}_3)$	1.480	1.472	
	$r(\text{SO}_4)$	1.480	1.472	
	$\angle\text{SO}_2\text{H}_2$	105.1	104.4	
	$\angle\text{O}_1\text{SO}_4$	115.7	115.7	
	$\angle\text{O}_1\text{SO}_3$	115.7	115.7	
	$\angle\text{O}_2\text{SO}_4$	103.9	103.9	
	$\mu$	2.46	2.77	
	$E$	-699.83676	-697.63776	

<sup>a</sup> Some of the atomic labels are omitted due to uniqueness or symmetry; atomic labels are in reference to Figure 1. <sup>b</sup> Experimental values for  $\text{NH}_3$  and  $\text{H}_2\text{O}$  are from ref 22, and for  $\text{H}_2\text{SO}_4$  from ref 23.

distance in the water dimer, 1.96 Å, a more typical hydrogen-bond distance. This indicates a very strong hydrogen bond between  $\text{H}_2\text{SO}_4$  and  $\text{NH}_3$ . The  $\text{O}_1\text{—H}_1$  covalent bond of  $\text{H}_2\text{SO}_4$  is not broken, but it is stretched to 1.043 Å from the equilibrium bond length of 0.970 Å for the isolated  $\text{H}_2\text{SO}_4$ . We attempted, but failed, to find the equilibrium geometry corresponding to the ionic  $\text{NH}_4^+\text{·HSO}_4^-$  system where the  $\text{O}_1\text{—H}_1$  covalent bond is completely broken and the proton ( $\text{H}_1$ ) is transferred from  $\text{H}_2\text{SO}_4$  to  $\text{NH}_3$ . To conclude, the  $\text{H}_2\text{SO}_4\text{—NH}_3$  system contains a strong hydrogen bond and no proton transfer takes place between  $\text{H}_2\text{SO}_4$  and  $\text{NH}_3$ .

Upon addition of a single water molecule to the system, the structure of the  $\text{H}_2\text{SO}_4\text{—NH}_3$  unit dramatically changes. Most noticeably, the bond distance  $r(\text{NH}_1)$  decreases by 0.480 Å to 1.106 Å, while the bond distance  $r(\text{O}_1\text{H}_1)$  increases by 0.421 Å to 1.464 Å (B3LYP). This indicates that the  $\text{O}_1\text{—H}_1$  bond is broken and a new  $\text{N—H}_1$  bond is formed. In other words, the transfer of a proton ( $\text{H}_1$ ) takes place from  $\text{H}_2\text{SO}_4$  to  $\text{NH}_3$ , resulting in the ion pair,  $\text{NH}_4^+\text{·HSO}_4^-$ . The water appears to stabilize the ion pair by hydrogen bonding to the  $\text{H}_5$  of  $\text{NH}_4^+$  (1.705 Å) and to the  $\text{O}_4$  of  $\text{HSO}_4^-$  (1.719 Å). Clearly, the polarity of the OH bond of  $\text{H}_2\text{O}$  plays a central role in the stabilization of the  $\text{NH}_4^+\text{·HSO}_4^-$  ion pair. Notice that these

**TABLE 2: Selected Equilibrium Bond Lengths (in Angstroms), Rotational Constants  $A$ ,  $B$ ,  $C$  (GHz), and Dipole Moments  $\mu$  (D) of the  $\text{H}_2\text{SO}_4\text{—NH}_3\text{—}(\text{H}_2\text{O})_n$  system from B3LYP and MP2 calculations with the 6-311++G(d,p) Basis Set**

parameter <sup>a</sup>	$\text{H}_2\text{SO}_4\text{—NH}_3$		$\text{H}_2\text{SO}_4\text{—NH}_3\text{—H}_2\text{O}$		$\text{H}_2\text{SO}_4\text{—NH}_3\text{—}(\text{H}_2\text{O})_2$	
	B3LYP	MP2	B3LYP	MP2	B3LYP	MP2
$r(\text{NH}_1)$	1.586	1.579	1.106	1.105	1.059	1.061
$r(\text{NH}_3)$	1.016	1.057	1.017	1.016	1.030	1.025
$r(\text{NH}_4)$	1.016	1.016	1.018	1.016	1.016	1.015
$r(\text{NH}_5)$	1.083	1.019	1.050	1.043	1.046	1.041
$r(\text{SO}_1)$	1.580	1.558	1.510	1.504	1.513	1.507
$r(\text{SO}_2)$	1.639	1.637	1.660	1.650	1.650	1.641
$r(\text{SO}_3)$	1.444	1.436	1.453	1.446	1.457	1.449
$r(\text{SO}_4)$	1.450	1.450	1.476	1.468	1.473	1.465
$r(\text{O}_1\text{H}_1)$	1.043	1.035	1.464	1.444	1.655	1.602
$r(\text{O}_2\text{H}_2)$	0.969	0.967	0.968	0.967	0.968	0.967
$r(\text{O}_4\text{H}_7)$			1.719	1.727	1.734	1.728
$r(\text{O}_5\text{H}_5)$			1.705	1.718	1.728	1.727
$r(\text{O}_6\text{H}_3)$					1.937	1.997
$r(\text{O}_1\text{H}_9)$					1.901	1.887
$A$	4.77948	4.80270	2.91831	2.93256	1.54673	1.54617
$B$	1.81905	1.87666	1.22958	1.28144	1.00396	1.02567
$C$	1.79618	1.86048	1.06114	1.09726	0.74425	0.75603
$\mu$	5.49	5.93	8.56	8.41	6.91	7.15

<sup>a</sup> Atomic labels are in reference to Figure 1.

**TABLE 3: Total Energies (hartrees), Binding Energies  $D_e$  (kcal/mol), Zero-Point Energy Corrections  $\Delta\text{ZPE}$  (kcal/mol), and ZPE-Corrected Binding Energies  $D_0$  (kcal/mol) of  $\text{H}_2\text{SO}_4\text{—NH}_3\text{—}(\text{H}_2\text{O})_n$  ( $n = 0, 1, 2$ ) from B3LYP and MP2 Calculations with the 6311++G(d,p) Basis Set**

system/theory	$E$	$D_e$	$\Delta\text{ZPE}$	$D_0$
$\text{H}_2\text{SO}_4\text{—NH}_3$				
B3LYP	-756.94814	16.49	-1.79	14.70
MP2	-754.37973	16.37	-1.69	14.69
$\text{H}_2\text{SO}_4\text{—NH}_3\text{—H}_2\text{O}$				
B3LYP	-833.42862	30.26	-4.90	25.37
MP2	-830.45000	30.99	-5.03	25.95
$\text{H}_2\text{SO}_4\text{—NH}_3\text{—}(\text{H}_2\text{O})_2$				
B3LYP	-909.90761	43.11	-7.84	35.27
MP2	-908.14406	44.94		

<sup>a</sup> Calculations were made with reference to isolated  $\text{H}_2\text{SO}_4$ ,  $\text{NH}_3$ , and  $\text{H}_2\text{O}$ .

hydrogen bond lengths involved with  $\text{H}_2\text{O}$  are considerably shorter than that in the water dimer.

The addition of a second water molecule further stabilizes the system. The  $r(\text{NH}_1)$  bond length decreases an additional 0.047 Å to 1.059 Å, while the  $r(\text{O}_1\text{H}_1)$  bond length increases by 0.191 Å to 1.655 Å (B3LYP). Despite these changes, the overall geometry of the  $\text{H}_2\text{SO}_4\text{—NH}_3$  unit with two water molecules is similar to that with one water molecule. In both cases proton transfer occurs and the ion pair is formed. No major structural changes are expected for the  $\text{H}_2\text{SO}_4\text{—NH}_3$  unit upon addition of three or more water molecules. Results from MP2 calculations are in general agreement with the B3LYP results discussed above.

**Binding Energies.** Table 3 presents the total energy  $E$  of each of the three clusters,  $\text{H}_2\text{SO}_4\text{—NH}_3\text{—}(\text{H}_2\text{O})_n$  ( $n = 0, 1, 2$ ). The binding energy  $D_e$  is determined as the difference between the total energy of the cluster and the sum of the total energies of the isolated monomers ( $\text{H}_2\text{SO}_4$ ,  $\text{NH}_3$ , and  $\text{H}_2\text{O}$ ) present in the cluster. The zero-point energy correction  $\Delta\text{ZPE}$  is added to  $D_e$  to give the ZPE-corrected binding energy  $D_0$ . The values of  $D_0$  calculated from B3LYP and MP2 theories are similar, deviating less than 3%. In the following discussion we will refer to the B3LYP results.

The binding energy,  $D_e$  or  $D_0$ , reveals the stability of the cluster as a result of intermolecular interactions and, for the



**TABLE 4: Harmonic Frequencies (cm<sup>-1</sup>) and Infrared Intensities (km/mol, in parentheses) of H<sub>2</sub>SO<sub>4</sub>–NH<sub>3</sub> Calculated from B3LYP and MP2 Calculations with the 6-311++G(d,p) Basis Set, Correlated by Intramolecular Vibrational Modes for NH<sub>3</sub> and H<sub>2</sub>SO<sub>4</sub>**

monomer mode	approximate description	separated monomers				H <sub>2</sub> SO <sub>4</sub> –NH <sub>3</sub> <sup>a</sup>	
		expt freq.	expt freq.	B3LYP	MP2	B3LYP	MP2
H <sub>2</sub> SO <sub>4</sub>							
<i>v</i> <sub>1</sub> (a)	OH stretch	3610 <sup>b,c</sup>	3563 (w) <sup>d</sup>	3761 (62)	3818 (71)	2505 (2889)	2538 (2863)
<i>v</i> <sub>2</sub> (a)	O=S=O sym stretch	1223 <sup>c</sup>	1216 (s)	1166 (147)	1216 (179)	1172 (213)	1215 (338)
<i>v</i> <sub>3</sub> (a)	S–(OH) <sub>2</sub> sym bend	1138	1136 (w)	1128 (96)	1135 (66)	1137 (141)	1165 (65)
<i>v</i> <sub>4</sub> (a)	S–(OH) <sub>2</sub> sym stretch	834	831 (m)	758 (130)	794 (147)	757 (180)	775 (198)
<i>v</i> <sub>5</sub> (a)	O=S=O bend	550	548 (s)	510 (49)	529 (61)	521 (20)	540 (20)
<i>v</i> <sub>6</sub> (a)	S–(OH) <sub>2</sub> bend	[372] <sup>e</sup>		358 (8)	377 (7)	365 (17)	395 (76)
<i>v</i> <sub>7</sub> (a)	torsion	[332]		314 (71)	325 (72)	1491 (114)	1513 (126)
<i>v</i> <sub>8</sub> (b)	antisym OH stretch	3610	3566 (vs)	3757 (196)	3813 (199)	3775 (110)	3829 (113)
<i>v</i> <sub>9</sub> (b)	antisym O=S=O stretch	1450	1452 (vs)	1414 (310)	1473 (317)	1348 (234)	1384 (269)
<i>v</i> <sub>10</sub> (b)	S–(OH) <sub>2</sub> antisym bend	1159	1157 (w)	1138 (85)	1147 (97)	1122 (36)	1124 (33)
<i>v</i> <sub>11</sub> (b)	S–(OH) <sub>2</sub> antisym stretch	883 <sup>c</sup>	882 (vs)	810 (353)	840 (358)	874 (284)	927 (233)
<i>v</i> <sub>12</sub> (b)	–OH wag	[675]		470 (51)	489 (55)	506 (28)	516 (50)
<i>v</i> <sub>13</sub> (b)	SO <sub>2</sub> rock	568	558 (s)	517 (21)	534 (25)	538 (47)	553 (21)
<i>v</i> <sub>14</sub> (b)	S–(OH) <sub>2</sub> rock	[422]		422 (30)	440 (32)	452 (12)	462 (21)
<i>v</i> <sub>15</sub> (b)	torsion			260 (78)	273 (67)	405 (83)	400 (25)
NH <sub>3</sub>							
<i>v</i> <sub>1</sub> ( <i>a</i> <sub>1</sub> )	sym stretch		3506 <sup>f</sup>	3480 (2)	3526 (2)	3466 (3)	3506.9 (2)
<i>v</i> <sub>2</sub> ( <i>a</i> <sub>1</sub> )	sym deformation		1022	1006 (214)	1073 (206)	1151 (253)	1204 (273)
<i>v</i> <sub>3</sub> ( <i>e</i> )	<i>d</i> -stretch		3577	3607 (8)	3678 (6)	3576 (34)	3640 (35)
						3594 (23)	3656 (28)
<i>v</i> <sub>4</sub> ( <i>e</i> )	<i>d</i> -deformation		1691	1669 (28)	1666 (24)	1662 (14)	1650 (12)
						1671 (22)	1652 (21)

<sup>a</sup> Intermolecular frequencies and IR intensities for H<sub>2</sub>SO<sub>4</sub>–NH<sub>3</sub> from B3LYP calculations: 43 (6), 95 (0), 100 (15), 236 (101), 263 (22), 347 (13); and from MP2 calculations: 36 (6), 90 (1), 102 (11), 178 (77), 264 (40), 350 (5). <sup>b</sup> Experimental harmonic frequencies for H<sub>2</sub>SO<sub>4</sub> vapor from ref 24. <sup>c</sup> Values refer to relative harmonic frequencies of Q branches. Harmonic frequencies (cm<sup>-1</sup>) of R and P branches are 3625, 3595 and 1236, 1209 and 895, 870, respectively. <sup>d</sup> Experimental harmonic frequencies and relative infrared intensities for H<sub>2</sub>SO<sub>4</sub> vapors trapped in argon matrixes from ref 25. <sup>e</sup> Experimental harmonic frequencies in brackets refer to liquid H<sub>2</sub>SO<sub>4</sub> from ref 24. <sup>f</sup> Experimental harmonic frequencies for NH<sub>3</sub> from ref 22.

larger clusters (*n* = 1 or 2), the proton-transfer reaction as well. The H<sub>2</sub>SO<sub>4</sub>–NH<sub>3</sub> cluster is very stable, as indicated by the large binding energy, *D*<sub>0</sub> = 14.70 kcal/mol (or *D*<sub>e</sub> = 16.49 kcal/mol). The typical hydrogen bond energy, such as in the water dimer, is *D*<sub>0</sub> = 3 to 4 kcal/mol.<sup>15</sup> This depicts a strong hydrogen-bond interaction between H<sub>2</sub>SO<sub>4</sub> and NH<sub>3</sub>, in agreement with the unusually short hydrogen-bond distance discussed earlier.

The effect of a single water molecule on the binding energy of the cluster H<sub>2</sub>SO<sub>4</sub>–NH<sub>3</sub>–H<sub>2</sub>O is notable. The binding energy of H<sub>2</sub>SO<sub>4</sub>–NH<sub>3</sub>–H<sub>2</sub>O is *D*<sub>0</sub> = 25.37 kcal/mol, an increase of 10.66 kcal/mol due to the addition of H<sub>2</sub>O. This large increase in *D*<sub>0</sub> is consistent with the equilibrium structure that, after the addition of a water molecule, proton transfer occurs and the ion pair forms. Without the presence of the ion pair, the increase in *D*<sub>0</sub> due to the water molecule would be considerably smaller because the formation of two typical hydrogen bonds by the added water would only contribute 6 to 8 kcal/mol to the *D*<sub>0</sub> value. It should be noted that the water molecule was placed in a position to provide the most stable interaction. Other possible positions of the water molecule relative to H<sub>2</sub>SO<sub>4</sub>–NH<sub>3</sub> were examined, but these configurations of the cluster were found less stable with significantly smaller binding energies. For example, when the water molecule accepts a hydrogen bond from the free OH group of sulfuric acid, the binding energy *D*<sub>e</sub> is 4.86 kcal/mol smaller than the most stable structure reported in Figure 2 and Table 3.

The addition of a second water molecule further increases the binding energy by 9.90 kcal/mol to 35.27 kcal/mol. This increase is again considerably larger than expected if no proton transfer had occurred in H<sub>2</sub>SO<sub>4</sub>–NH<sub>3</sub> and two typical hydrogen bonds were formed by the second water. The large increase in *D*<sub>0</sub> is therefore consistent with the equilibrium structure where the second water, just as the first water, is present to support the NH<sub>4</sub><sup>+</sup>·HSO<sub>4</sub><sup>-</sup> ion pair, yielding significant stabilization of

the system. Both of the increases in *D*<sub>0</sub>, due to consecutive addition of two water molecules, are also reflected in the equilibrium structures where the hydrogen bonds involved with the water molecules are shorter than typical, such as in the water dimer. If the second water was positioned to accept a hydrogen bond from the free OH group of HSO<sub>4</sub><sup>-</sup>, the configuration would be significantly less stable and the binding energy increase would be smaller for the same reason as discussed for the H<sub>2</sub>SO<sub>4</sub>–NH<sub>3</sub>–H<sub>2</sub>O cluster.

**Harmonic Frequencies.** Table 4 presents the harmonic vibrational frequencies and infrared intensities of the H<sub>2</sub>SO<sub>4</sub>–NH<sub>3</sub> cluster, with all of the intramolecular modes correlated by the monomer vibrations of H<sub>2</sub>SO<sub>4</sub> and NH<sub>3</sub>. Similarly, Table 5 presents the harmonic frequencies and infrared intensities of the larger clusters, H<sub>2</sub>SO<sub>4</sub>–NH<sub>3</sub>–H<sub>2</sub>O and H<sub>2</sub>SO<sub>4</sub>–NH<sub>3</sub>–(H<sub>2</sub>O)<sub>2</sub>, with all of the intramolecular modes correlated by the monomers H<sub>2</sub>SO<sub>4</sub><sup>-</sup>, NH<sub>4</sub><sup>+</sup>, and H<sub>2</sub>O. The intermolecular harmonic frequencies and infrared intensities are given in the footnotes of Tables 4 and 5. The available experimental frequencies<sup>22,24–27</sup> are given along with the calculated harmonic frequencies and infrared intensities.

The B3LYP and MP2 values of the harmonic frequencies and infrared intensities for the monomers and clusters are consistent, with the B3LYP frequencies being slightly (1–5%) lower than the corresponding MP2 values. It is known that MP2 harmonic frequencies are generally overestimated by as much as 10% as compared to experimental harmonic frequencies. As a result, our B3LYP harmonic frequencies are perhaps more accurate and will be used for our following discussion. As shown in Table 4, the B3LYP harmonic frequencies of the monomers are typically within 10% of the available experimental values. No experimental harmonic frequencies are available for the gas-phase ions HSO<sub>4</sub><sup>-</sup> and NH<sub>4</sub><sup>+</sup>. However, the fundamental frequencies of the NH<sub>4</sub><sup>+</sup> ion, as determined from the infrared

**TABLE 5: Harmonic Frequencies ( $\text{cm}^{-1}$ ) and Infrared Intensities ( $\text{km/mol}$ , in parentheses) of  $\text{H}_2\text{SO}_4\text{-NH}_3\text{-H}_2\text{O}$  and  $\text{H}_2\text{SO}_4\text{-NH}_3\text{-(H}_2\text{O)}_2$  Calculated from B3LYP and MP2 Calculations with the 6-311++G(d,p) Basis Set, Correlated by Intramolecular Vibrational Modes for  $\text{HSO}_4^-$ ,  $\text{NH}_4^+$ , and  $\text{H}_2\text{O}$** 

monomer mode	separated monomers			$\text{H}_2\text{SO}_4\text{-NH}_3\text{-H}_2\text{O}^a$		$\text{H}_2\text{SO}_4\text{-NH}_3\text{-(H}_2\text{O)}_2^b$
	expt freq.	B3LYP	MP2	B3LYP	MP2	B3LYP
$\text{HSO}_4^-$						
$\nu_1$		136 (67)	159 (65)	182 (57)	201 (6)	188 (41)
$\nu_2$		368 (14)	382 (4)	366 (5)	388 (14)	388 (27)
$\nu_3$		398 (13)	411 (13)	399 (22)	411 (43)	420 (21)
$\nu_4$		508 (4)	528 (7)	548 (32)	556 (46)	532 (40)
$\nu_5$		527 (30)	545 (31)	569 (41)	583 (55)	568 (28)
$\nu_6$		538 (44)	556 (52)	636 (30)	637 (43)	606 (40)
$\nu_7$		670 (300)	689 (320)	741 (241)	765 (255)	746 (159)
$\nu_8$		989 (92)	1037 (84)	971 (415)	1007 (443)	981 (335)
$\nu_9$		1109 (101)	1120 (91)	1096 (324)	1121 (151)	1109 (290)
$\nu_{10}$		1181 (424)	1233 (460)	1129 (156)	1152 (325)	1141 (187)
$\nu_{11}$		1241 (362)	1286 (411)	1292 (441)	1345 (478)	1286 (374)
$\nu_{12}$		3810 (29)	3862 (35)	3792 (91)	3839 (93)	3789 (88)
$\text{NH}_4^+$						
$\nu_1 (a_1)$	3115 <sup>c</sup>	3371 (0)	3414 (0)	3510 (63)	3565 (89)	3345 (238)
$\nu_2 (e)$	1638	1727 (0)	1734 (0)	1723 (5)	1747 (4)	1726 (44)
				1754 (91)	1771 (105)	1768 (33)
$\nu_3 (t)$	3250	3475 (183)	3548 (195)	2157 (2461)	2167 (2605)	2850 (1086)
				2995 (794)	3121 (692)	3053 (696)
				3580 (58)	3646 (67)	3565 (88)
$\nu_4 (t)$	1398	1490 (163)	1496 (155)	1380 (13)	1387 (9)	1408 (82)
				1534 (130)	1545 (112)	1518 (93)
				1587 (88)	1617 (88)	1581 (206)
$\text{H}_2\text{O}$						
$\nu_1 (a_1)$	3832 <sup>d</sup>	3817 (9)	3884 (13)	3403 (1098)	3524 (942)	3592 (572)
						3442 (1012)
$\nu_2 (a_2)$	3943	3922 (57)	4003 (63)	3892 (94)	3915 (105)	3903 (103)
						3894 (98)
$\nu_3 (b_1)$	1648	1603 (67)	1629 (57)	1646 (50)	1675 (55)	1636 (46)
						1656 (27)

<sup>a</sup> Intermolecular frequencies and IR intensities for  $\text{H}_2\text{SO}_4\text{-NH}_3\text{-H}_2\text{O}$  from B3LYP calculations: 24 (3), 36 (6), 97 (10), 201 (8), 212 (111), 216 (57), 282 (69), 326 (126), 417 (5), 492 (184), 532 (21), 821 (152); and from MP2 calculations: 23 (4), 33 (5), 90 (9), 214 (42), 237 (65), 259 (64), 311 (95), 328 (162), 434 (0), 497 (142), 552 (42), 827 (173). <sup>b</sup> Intermolecular frequencies and IR intensities for  $\text{H}_2\text{SO}_4\text{-NH}_3\text{-(H}_2\text{O)}_2$  from B3LYP calculations: 20 (4), 43 (6), 55 (1), 85 (8), 139 (128), 158 (26), 177 (16), 207 (56), 221 (97), 278 (81), 301 (91), 334 (19), 376 (8), 458 (80), 491 (216), 550 (68), 644 (85), 775 (208). <sup>c</sup> Experimental fundamental frequencies measured for  $\text{NH}_4^+$  in solid ammonium metavanadate ( $\text{NH}_4\text{VO}_3$ ) from ref 26. <sup>d</sup> Experimental harmonic frequencies for  $\text{H}_2\text{O}$  from ref 27.

spectra of solid ammonium metavanadate ( $\text{NH}_4\text{VO}_3$ ),<sup>26</sup> indicate that the calculated harmonic frequencies for  $\text{NH}_4^+$  agree very well with the experimental fundamental frequencies.

Most of the harmonic frequencies of the intramolecular modes of the  $\text{H}_2\text{SO}_4\text{-NH}_3$  cluster are nearly the same as those of the isolated monomers  $\text{H}_2\text{SO}_4$  and  $\text{NH}_3$ . Despite the lifting of the degeneracy in the d-stretch ( $\nu_3$ ) and d-deformation ( $\nu_4$ ) modes of  $\text{NH}_3$ , the frequency shifts due to complexation tend to fall within 5% of the monomer frequencies. This further confirms that the  $\text{H}_2\text{SO}_4\text{-NH}_3$  cluster does not undergo significant changes in chemical bonding from its isolated monomers. However, two large frequency shifts must be noted, both of which involve the proton  $\text{H}_1$  of  $\text{H}_2\text{SO}_4$ . The first frequency shift is for the OH stretching mode ( $\nu_1$ ) of  $\text{H}_2\text{SO}_4$ . The  $\text{O}_1\text{-H}_1$  stretch mode undergoes a red-shift of  $1256 \text{ cm}^{-1}$  at the B3LYP level, from a frequency of  $3761 \text{ cm}^{-1}$  for the monomer to  $2505 \text{ cm}^{-1}$  for the cluster. This exceptionally large red-shift is accompanied by a huge enhancement in the IR activity. The IR intensity of the OH stretch mode is enhanced by more than an order of magnitude, from  $62 \text{ km/mol}$  for the monomer to  $2889 \text{ km/mol}$  for the cluster. This indicates a considerable weakening in the  $\text{O}_1\text{-H}_1$  bond of  $\text{H}_2\text{SO}_4$  as a result of its formation of a hydrogen bond with  $\text{NH}_3$ . Similar frequency shifts and IR enhancement are obtained from MP2 theory. It should be noted that the OH stretching mode ( $\nu_1$ ) of the  $\text{H}_2\text{SO}_4\text{-NH}_3$  cluster is useful in a spectroscopic search. Not only is the IR intensity very large, but also the frequency of  $2505 \text{ cm}^{-1}$  (from B3LYP theory) is considerably separated from all other frequencies of the cluster.

The second noteworthy frequency shift due to complexation is for the torsional mode ( $\nu_7$ ) of the  $\text{H}_2\text{SO}_4\text{-NH}_3$  cluster. The frequency of  $\nu_7$  increases from  $314 \text{ cm}^{-1}$  for the monomer to  $1491 \text{ cm}^{-1}$  for the complex. This torsional mode is mainly an out-of-plane motion of the covalently bonded  $\text{H}_1$  in the  $\text{H}_2\text{SO}_4$  monomer. In the complex,  $\text{H}_1$  is also bound to  $\text{NH}_3$  via a strong hydrogen bond. The hydrogen bonding is expected to significantly enhance the force constant for the out-of-plane motion of  $\text{H}_1$  and result in a large blue-shift for the torsional mode ( $\nu_7$ ) of  $\text{H}_2\text{SO}_4$ . Clearly this analysis gives a reasonable explanation for the large blue-shift of  $\nu_7$ . It should be added that the large blue-shift of  $\nu_7$  is also indicative of the strongly directional hydrogen bond in  $\text{H}_2\text{SO}_4\text{-NH}_3$ .

The harmonic frequencies of the larger clusters,  $\text{H}_2\text{SO}_4\text{-NH}_3\text{-H}_2\text{O}$  and  $\text{H}_2\text{SO}_4\text{-NH}_3\text{-(H}_2\text{O)}_2$  (Table 5), are considerably different from those of the  $\text{H}_2\text{SO}_4\text{-NH}_3$  cluster. The frequencies of the intramolecular modes are difficult to correlate with those of the  $\text{H}_2\text{SO}_4$  and  $\text{NH}_3$  monomers, but are relatively easy to correlate with those of the separate  $\text{HSO}_4^-$  and  $\text{NH}_4^+$  ions and  $\text{H}_2\text{O}$ . For example, only one OH stretch frequency, attributed to the free OH group of the bisulfate ion, exists in each of these larger clusters. The B3LYP frequencies,  $3792$  and  $3789 \text{ cm}^{-1}$  for  $\text{H}_2\text{SO}_4\text{-NH}_3\text{-H}_2\text{O}$  and  $\text{H}_2\text{SO}_4\text{-NH}_3\text{-(H}_2\text{O)}_2$ , respectively, are comparable to the frequency of  $3810 \text{ cm}^{-1}$  for the isolated  $\text{HSO}_4^-$  ion. The frequency above  $2000 \text{ cm}^{-1}$  for the stretch of the OH bonded to  $\text{NH}_3$  in the  $\text{H}_2\text{SO}_4\text{-NH}_3$  cluster is absent in the larger clusters. This further supports our earlier conclusion that the ion pair  $\text{NH}_4^+\text{HSO}_4^-$  is formed in the larger

clusters. As expected, however, the frequencies of the ions in the complexes are not exactly the same as those of the isolated ions, due to interactions among the ions and H<sub>2</sub>O in the clusters. The lower frequencies, particularly for HSO<sub>4</sub><sup>−</sup>, are difficult to assign. The largest frequency shifts appear to be related to the reduction of symmetry of the NH<sub>4</sub><sup>+</sup> ion. For example, from B3LYP theory, the frequency of the 3-fold degenerate stretching mode of the NH<sub>4</sub><sup>+</sup> ion is split from  $\nu_7(t) = 3475 \text{ cm}^{-1}$  in the isolated ion to 2157, 2995, and 3580  $\text{cm}^{-1}$  in H<sub>2</sub>SO<sub>4</sub>–NH<sub>3</sub>–H<sub>2</sub>O and 2850, 3053, and 3565  $\text{cm}^{-1}$  in H<sub>2</sub>SO<sub>4</sub>–NH<sub>3</sub>–(H<sub>2</sub>O)<sub>2</sub>. The antisymmetric stretch mode is assigned to the frequency with the largest red-shift: 2157  $\text{cm}^{-1}$  in H<sub>2</sub>SO<sub>4</sub>–NH<sub>3</sub>–H<sub>2</sub>O, and 2850  $\text{cm}^{-1}$  in H<sub>2</sub>SO<sub>4</sub>–NH<sub>3</sub>–(H<sub>2</sub>O)<sub>2</sub>. This stretch mode corresponds to the transfer of a proton H<sub>1</sub> from NH<sub>4</sub><sup>+</sup> to HSO<sub>4</sub><sup>−</sup>, and is an exact reverse of the proton transfer from H<sub>2</sub>SO<sub>4</sub> to NH<sub>3</sub>. The large red-shift is accompanied by a large increase in IR intensity, which is similar to the O<sub>1</sub>–H<sub>1</sub> stretch of H<sub>2</sub>SO<sub>4</sub> discussed earlier for the H<sub>2</sub>SO<sub>4</sub>–NH<sub>3</sub> cluster.

With the effect of water on H<sub>2</sub>SO<sub>4</sub>–NH<sub>3</sub> established, we turn our attention to the harmonic frequencies associated with the H<sub>2</sub>O molecules themselves. Although the  $\nu_2$  (antisymmetric stretch) and  $\nu_3$  (bend) modes of H<sub>2</sub>O change very little upon addition to the H<sub>2</sub>SO<sub>4</sub>–NH<sub>3</sub> cluster, a marked change is noted for the  $\nu_1$  (symmetric stretch) mode. A large red-shift is seen in the  $\nu_1$  mode, along with a sharp enhancement of IR intensity. Clearly, not only do the water molecules affect the H<sub>2</sub>SO<sub>4</sub>–NH<sub>3</sub> cluster, enabling the formation of HSO<sub>4</sub><sup>−</sup> and NH<sub>4</sub><sup>+</sup> ions, but also the water molecules themselves are affected by the ions formed. This mutual influence and interaction between H<sub>2</sub>O and H<sub>2</sub>SO<sub>4</sub>–NH<sub>3</sub> may be valuable in the understanding of the strong nonideality and other related properties of some aqueous solutions. Continuum models based upon the self-consistent reaction field (SCRf) theory are limited in their inability to provide the detailed information about solvent–solute effects, such as described here.

Finally, the intermolecular harmonic frequencies and IR intensities are listed in the footnotes of Tables 4 and 5. The number of intermolecular vibrational modes rapidly increases from 6 to 12 to 18 for the clusters with the number of water molecules  $n = 0, 1,$  and  $2,$  respectively. In general, no clear descriptions for the intermolecular vibrational modes are available due to the mixing with intramolecular modes. However, some trends are evident. The highest frequencies are from the in-plane distortions and the next are for out-of-plane distortions, all with respect to the planes established by hydrogen-bonded ring structures. The lowest frequencies are normally for rotations of submolecules about the axes connecting to other submolecules in the cluster, on the condition that such rotations are not hindered by constraints from hydrogen bonding.

## Conclusions and Remarks

The proton-transfer reaction of sulfuric acid–ammonia and the effect of the first two water molecules have been studied by density functional theory and ab initio molecular orbital theory. The equilibrium structures, binding energies, harmonic frequencies, and other molecular properties of the clusters H<sub>2</sub>SO<sub>4</sub>–NH<sub>3</sub>–(H<sub>2</sub>O)<sub>*n*</sub> ( $n = 0, 1, 2$ ) were calculated at the B3LYP and MP2 levels with the 6-311++G(d,p) basis set. The B3LYP and MP2 calculations gave consistent results. Without water, the sulfuric acid–ammonia system was determined to be only hydrogen bonded, with sulfuric acid acting as the hydrogen-bond donor and ammonia as the acceptor. No energy minimum

was found to correspond to the NH<sub>4</sub><sup>+</sup>·H<sub>2</sub>SO<sub>4</sub><sup>−</sup> ion pair that would result if a proton-transfer had occurred in H<sub>2</sub>SO<sub>4</sub>–NH<sub>3</sub>. In the presence of one or two water molecules, however, the H<sub>2</sub>SO<sub>4</sub>–NH<sub>3</sub> system exists only as the NH<sub>4</sub><sup>+</sup>·H<sub>2</sub>SO<sub>4</sub><sup>−</sup> ion pair that results from a complete proton transfer from sulfuric acid to ammonia. The analysis of selected equilibrium bond lengths, binding energies, and harmonic frequencies of the clusters provided strong support for a complete proton transfer in the presence of one or two water molecules.

The relative acidity of acid molecules appears to be correlated to the minimum number of water molecules required to allow proton transfer from the acid to NH<sub>3</sub>. Nitric acid (HNO<sub>3</sub>) and hydrogen chloride (HCl) are weaker in acidity than H<sub>2</sub>SO<sub>4</sub>, and both HNO<sub>3</sub>–NH<sub>3</sub> and HCl–NH<sub>3</sub> require at least two water molecules to allow the proton transfer to occur.<sup>6,7</sup> In this paper we have shown that only one water molecule is required for proton transfer in H<sub>2</sub>SO<sub>4</sub>–NH<sub>3</sub>.

The result of this study may have significant implications in atmospheric chemistry. In particular, it may provide new insights in understanding the key step in the formation of sulfate-containing aerosols from homogeneous gas-phase species. As shown by this study, sulfuric acid and ammonia are paired to form a hydrogen-bonded complex without water, but they transform into an ion pair in the presence of a single water molecule. Under normal atmospheric conditions with sufficient H<sub>2</sub>O vapor pressure, sulfuric acid can readily absorb ammonia to produce ammonium bisulfate. On the other hand, in extremely dry conditions, sulfuric acid is dehydrated and it only forms a hydrogen-bonded complex with ammonia.

**Acknowledgment.** This work was supported in part by The Petroleum Research Fund of The American Chemical Society (ACS-PRF Grant No. 30399-GB6) and by The Research Corporation (CC4121).

## References and Notes

- Castleman, A. W.; Dans, R. E.; Mukelwitz, H. R.; Tang, I. N.; Wood, W. P. *Int. J. Chem. Kinet. Symp.* **1975**, *1*, 629.
- Seinfeld, J. H. *Atmospheric Chemistry and Physics of Air Pollution*; Wiley: New York, 1986; p 738.
- Pueschel, R. F. *Composition, Chemistry, and Climate of the Atmosphere*; Singh, H. B., Ed.; Van Nostrand Reinhold: New York, 1995; p 126.
- Berresheim, H.; Wine, P. H.; Davis, D. D. *Composition, Chemistry, and Climate of the Atmosphere*; Singh, H. B., Ed.; Van Nostrand Reinhold: New York, 1995; pp 296–299.
- Nguyen, M.-T.; Jamka, A. J.; Cazar, R. A.; Tao, F.-M. *J. Chem. Phys.* **1997**, *106*, 8710.
- Tao, F.-M. *J. Chem. Phys.* **1998**, *108*, 193.
- Cazar, R. A.; Jamka, A. J.; Tao, F.-M. *J. Phys. Chem. A* **1998**, *102*, 5117.
- Becke, A. D. *J. Chem. Phys.* **1992**, *96*, 2155.
- Becke, A. D. *J. Chem. Phys.* **1992**, *97*, 9193.
- Becke, A. D. *J. Chem. Phys.* **1993**, *98*, 5648.
- Lee, C.; Yang, W.; Parr, R. G. *Phys. Rev. B* **1988**, *37*, 785.
- Møller, C.; Plesset, M. J. *Phys. Rev.* **1934**, *26*, 618.
- Brinkley, J. S.; Pople, J. A. *Int. J. Quantum Chem.* **1975**, *9*, 229.
- Kim, K.; Jordan, K. D. *J. Phys. Chem.* **1994**, *98*, 10089.
- Rablen, P. R.; Lockman, J. W.; Jorgensen, W. L. *J. Phys. Chem. A* **1998**, *102*, 3782.
- Krishnan, R.; Brinkley, J. S.; Seeger, R.; Pople, J. A. *J. Chem. Phys.* **1980**, *72*, 650.
- Frisch, M. J.; Pople, J. A.; Brinkley, J. S. *J. Chem. Phys.* **1984**, *80*, 3265.
- Clark, T.; Chandrasekhar, J.; Spitznagel, G. W.; Schleyer, P. v. R. *J. Comput. Chem.* **1983**, *4*, 294.
- Hehre, W. J.; Random, L.; Schleyer, P. v. R.; Pople, J. A. *Ab Initio Molecular Orbital Theory*; Wiley: New York, 1986.
- Frisch, M. J.; Trucks, G. W.; Schlegel, H. B.; Gill, P. M. W.; Johnson, B. G.; Robb, M. A.; Cheeseman, J. R.; Keith, T.; Petersson, G. A.; Montgomery, J. A.; Raghavachari, K.; Al-Laham, M. A.; Zakrzewski,

V. G.; Ortiz, J. V.; Foresman, J. B.; Cioslowski, J.; Stefanov, B. B.; Nanayakkara, A.; Challacombe, M.; Peng, C. Y.; Ayala, P. Y.; Chen, W.; Wong, M. W.; Andres, J. L.; Replogle, E. S.; Gomperts, R.; Martin, R. L.; Fox, D. J.; Binkely, J. S.; Defress, D. J.; Baker, J.; Stewart, J. P.; Head-Gordon, M.; Gonzalez, C.; Pople, J. A. *Gaussian 94*, Revision D.3; Gaussian, Inc.: Pittsburgh, PA, 1995.

(21) Frisch, M. J.; Trucks, G. W.; Schlegel, H. B.; Scuseria, G. E.; Robb, M. A.; Cheeseman, J. R.; Zakrzewski, V. G.; Montgomery, J. A., Jr.; Stratmann, R. E.; Burant, J. C.; Dapprich, S.; Millam, J. M.; Daniels, A. D.; Kudin, K. N.; Strain, M. C.; Farkas, O.; Tomasi, J.; Barone, V.; Cossi, M.; Cammi, R.; Mennucci, B.; Pomelli, C.; Adamo, C.; Clifford, S.; Ochterski, J.; Petersson, G. A.; Ayala, P. Y.; Cui, Q.; Morokuma, K.; Malick, D. K.; Rabuck, A. D.; Raghavachari, K.; Foresman, J. B.; Cioslowski, J.; Ortiz, J. V.; Stefanov, B. B.; Liu, G.; Liashenko, A.; Piskorz, P.; Komaromi, I.; Gomperts, R.; Martin, R. L.; Fox, D. J.; Keith, T.; Al-Laham, M. A.; Peng, C. Y.; Nanayakkara, A.; Gonzalez, C.; Challacombe, M.; Gill, P. M.

W.; Johnson, B.; Chen, W.; Wong, M. W.; Andres, J. L.; Gonzalez, C.; Head-Gordon, M.; Replogle, E. S.; Pople, J. A. *Gaussian 98*, Revision A.2; Gaussian, Inc.: Pittsburgh, PA, 1998.

(22) Huber K. P.; Herzberg, G. *Molecular Spectra and Molecular Structure, V. Constants of Polyatomic Molecules*; Van Nostrand Reinhold: New York, 1979.

(23) *CRC Handbook of Chemistry and Physics*, 77<sup>th</sup> ed.; Lide, D. R., Ed.; 1996; pp 9–19.

(24) Chakcalackal, S. M.; Stafford, F. E. *J. Am. Chem. Soc.* **1966**, *88*, 723.

(25) Givan, A.; Larsen, L.; Loewenschuss, A.; Nielsen, C. J. *J. Chem. Soc., Faraday Trans.* **1998**, *94* (7), 827.

(26) de Waal, D.; Heyns, A. M.; Range, K.-J.; Eglmeier, C. *Spectrochim. Acta* **1990**, *46A*, 1639.

(27) Strey, G. *J. Mol. Spectrosc.* **1967**, *24*, 87.